Available online at www.sciencedirect.com
SCIENCE DIRECT®
Journal of Nuclear Materials 329–333 (2004) 81–87
journal of nuclear materials
www.elsevier.com/locate/jnucmat

Analysis of defect structural evolution in fcc metals irradiated with neutrons under well defined boundary conditions

T. Yoshiie [a,*], Y. Satoh [b], Q. Xu [a]

[a] Research Reactor Institute, Kyoto University, Kumatori, Osaka 590-0494, Japan
[b] Institute for Materials Research, Tohoku University, Katahira, Aoba-ku, Sendai 980-8577, Japan

Abstract

Defect structural evolutions near pre-existing defects such as surfaces, grain boundaries and dislocations in fcc metals are studied to clarify point defect processes during irradiation. By the comparison of Au irradiated as thin foils with fission neutrons and fusion neutrons, the PKA energy to produce a stacking fault tetrahedron is determined to be 80 keV with a production efficiency of 0.05. Grain boundaries are effectively used to detect the existence of one-dimensional motion of interstitial clusters. In Ni and Ni binary alloys (2 at.% Si, Cu, Ge or Sn), there is a good coincidence between the void growth and one-dimensional motion of interstitial clusters. The coincidence is, however, not good for Cu. Screw dislocations with jogs turn into helical dislocations by absorbing one type of point defects. The difference of freely migrating defects between fission and fusion neutron irradiation is measured as a function of irradiation dose and it is concluded that the same number of freely migrating defects is generated from each subcascade in fission and fusion neutron irradiated Ni.

1. Introduction

Freely migrating defects are annihilated at permanent sinks. Therefore the defect structural evolution is affected remarkably by the presence of sinks. The sinks are considered to be a boundary condition of diffusion problem and an analysis including the boundary condition gives us a lot of information for damage structural evolution.

Professor Kiritani was the first researcher who realized the importance of sink geometries for the materials irradiation experiments. He compared the difference of the damage structures in thin foil irradiation and bulk irradiation [1]. In thin foil irradiation, specimens are irradiated after polishing for electron microscopy observation. He obtained information about defect clusters formed directly by a single cascade event. The result of bulk irradiation in which specimens are polished after irradiation for electron microscopy observation indicated the effect of freely migrating defects. We have developed and expanded his idea and used pre-existing defects such as dislocations and grain boundaries (GB) as well as surfaces to detect point defect processes during irradiation. In this paper, results on the analysis of defect structural evolution near pre-existing defects in FCC metals are presented.

2. Fission–fusion correlation of damage structures in Au

Surfaces and GB are important sinks for freely migrating defects produced by irradiation. Near such sinks, most of freely migrating defects are captured by the sink. If stacking fault tetrahedra (SFTs) are formed directly in the cascades and interstitials and their clusters

* Corresponding author. Tel.: +81-724 51 2473; fax: +81-724 51 2620.
E-mail address: yoshiie@rri.kyoto-u.ac.jp (T. Yoshiie).

0022-3115/$ - see front matter © 2004 Elsevier B.V. All rights reserved.
doi:10.1016/j.jnucmat.2004.04.006

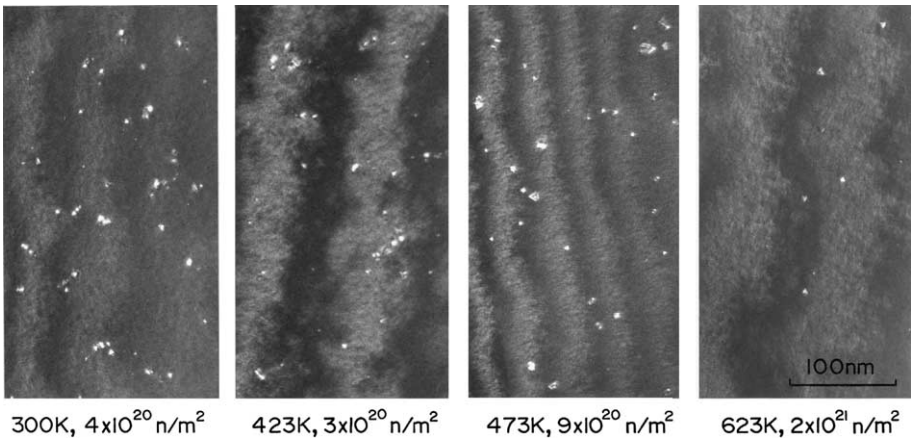

Fig. 1. Damage structures in Au after D-T fusion neutron irradiation using RTNS-II as thin foils.

escape to the surfaces in thin foil specimens, cascade structures are retained. At lower temperatures the subcascade structure is observed [1]. In the case of compact cascade such as those produced in Au, with increasing irradiation temperatures, above 473 K, well separated subcascades (SFTs) fuse into a large SFT as shown in Fig. 1. Average SFT sizes irradiated at 300 and 473 K were 1.6 and 3.7 nm, respectively. Above 623 K only few SFTs remain due to their thermal unstableness. The SFT size is larger for larger PKA energy. Fig. 2 shows the comparison of defect structures between fission neutron irradiation (the JMTR, 573 K, 0.044 dpa) and fusion neutron irradiation (the RTNS-II, 563 K, 0.017 dpa). Though the total displacement damage for the fission neutron irradiation is higher than that of the fusion neutron irradiation, the remaining number of SFTs is higher in the fusion neutron irradiation. The cross-section for the formation of SFTs is 1.7×10^{-1} b and 9.4×10^{-4} b for fusion neutrons and fission neutrons, respectively. The average size of SFTs by fusion neutron irradiation is also larger than that of fission neutron irradiation. If there exists a threshold energy for SFT formation (E_{TH}), it is evaluated using the following equation,

$$N_{SFT} = \alpha\varphi \int_{E_{TH}}^{\infty} \frac{d\sigma(E)}{dE}\, dE,$$

where N_{SFT} is the concentration of SFTs observed, α is the SFT formation efficiency, φ is the total neutron fluence and $\frac{d\sigma}{dE}$ is the differential cross-section of incident neutrons that collide to transfer an amount of energy E. We adopted the cross-section calculated by the SPECTER code [2] using the neutron spectrum of the JMTR. α and E_{TH} are obtained to be 0.05 and 80 keV, respectively, using the number density of SFTs formed by fission neutron irradiation and fusion neutron irradiation with fitting accuracy of 10%. It is concluded that SFTs are formed for PKA energies larger than 80 keV with a cascade efficiency of 0.05 at 563–573 K. Actually α depends on the PKA energy, so the value is an average one above 80 keV.

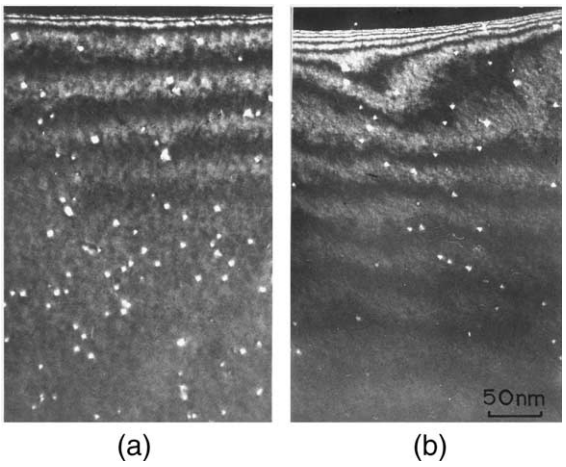

Fig. 2. Damage structures in Au: (a) after fusion neutron irradiation in the RTNS-II for 0.017 dpa at 563 K and (b) after fission neutron irradiation in the JMTR for 0.044 dpa at 573 K. Both were irradiated as thin foils.

3. Damage structural evolution as a function of the specimen thickness

With increasing distance to the surface, freely migrating defects formed by cascade damage are increasingly unlikely to escape to the surface and interactions increase between defects produced by displacement damage. Fig. 3 shows the defect structural evolution of fission neutron irradiated Ni–0.05 at.% Ge

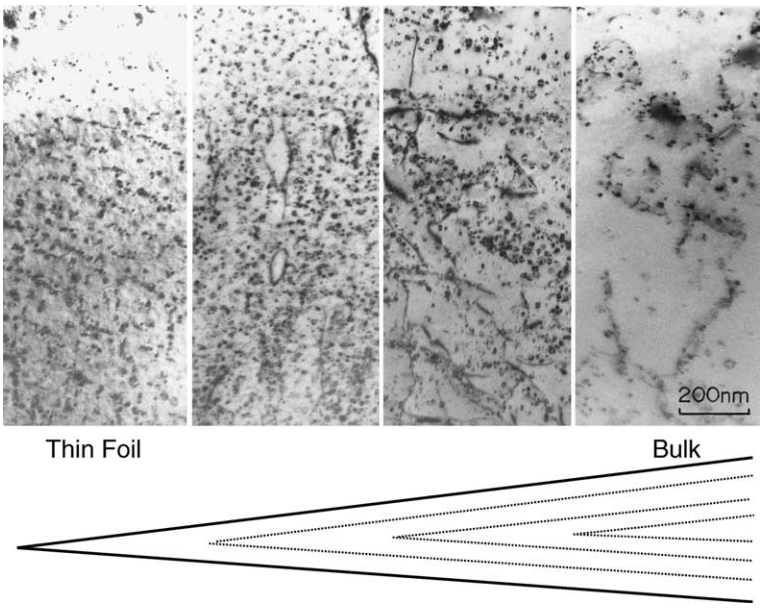

Fig. 3. The thickness dependence of defect structures in fission neutron irradiated Ni–0.05 at.% Ge at 573 K to 0.11 dpa. The specimen was irradiated as thin foil and observed (left panel). The right three panels were observed after successive polishing to reveal initially thicker regions of the irradiated foil.

to a dose of 0.11dpa at 573 K. The specimen was irradiated as a thin foil. In thin regions, defect clusters, 60% of interstitial type dislocation loops and 40% of SFTs, are observed as shown in the left panel of Fig. 3. By successive polishing of the specimen, observation of thicker regions is possible as illustrated in the lower figure. The right three panels of Fig. 3 show the microstructure after removal of about 100, 500 and 2000 nm from each surface. The coalescence of loops and formation of dislocation net-works are observed. Voids are also observed between dislocations in the right panel. If we consider that the concentration of freely migrating defects is low near surfaces, the panels from the left to the right in Fig. 3 indicate the defect structural evolution as a function of freely migrating defects. This irradiation was performed with conventional temperature control, where the specimen temperature was increased with neutron flux [3]. The interstitial type dislocation loops near the surface were mainly formed during the irradiation at low temperatures. No loops were observed in thin foil specimens with controlled irradiation at 573 K in Ni and Ni–0.05 at.% dilute alloys.

4. Void growth and movement of interstitial clusters

4.1. Defect structures near GB

The importance of one-dimensional motion of interstitial clusters on microstructural evolution in metals has been pointed out by many researchers [4–9]. GB can be effectively used in order to detect the existence of one-dimensional motion of interstitial clusters. Interstitial type dislocation loops are not formed near GB when interstitial clusters are mobile because of their easy escape to GB This is clearly shown by a reaction kinetics analysis, which includes the point defect and cluster flow into planar sink (GB). The results are shown in Fig. 4, for three cases. The values of parameters are the same as those in the previous papers simulating the irradiation of Ni using the JMTR at 573 K to 0.2 dpa [10,11]. The ratio of interstitial clusters formed directly in cascades to the total interstitials is determined to be 5×10^{-6} to fit the experimental result. The point defect flow into the planar sink is taken into equations as boundary conditions, i.e., the concentration of point defects and their clusters is zero at the planar sink. (a) in Fig. 4 is the system containing the formation of immobile interstitial clusters (loops) and voids. Voids and loops grow in the matrix and the growth of loops is pronounced near the planar sink. In this system, as a result of the growth of loops, excess vacancies accumulate in voids in the matrix. Near the planar sink, vacancies can escape there, and accordingly more loops remain. If we introduce the motion of interstitial clusters in this system, the loops near GB decrease as shown (b) in Fig. 4, where the mobility of interstitial clusters was taken as the 10^{-4} of an interstitial mobility. In the system in which only the formation of immobile interstitial clusters is assumed,

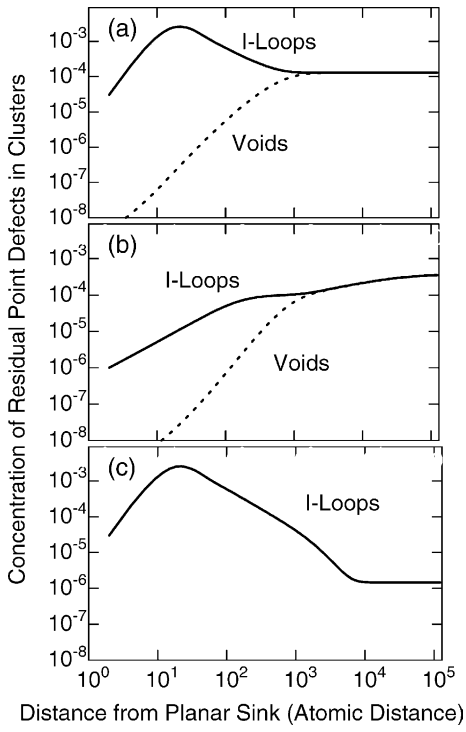

Fig. 4. Calculation of residual point defects in clusters after irradiation of 0.2 dpa at 573 K as a function of the distance from the GB measured by a unit of atomic distance (distance between two atoms). (a) is for coexisting interstitial clusters (dislocation loops) and voids. The migration of interstitial clusters is not introduced. (b) is the same system as (a) and the migration of interstitial clusters is introduced. (c) is the case when only interstitial clusters (loops) exist. The migration of interstitial clusters is not introduced.

loops preferentially grow in a narrow volume near the planar sink as shown in Fig. 4(c). Vacancies produced in the matrix are absorbed by loops because of no formation of vacancy clusters, reducing the number of interstitials in loops.

Ni and four kinds of Ni alloys, 2 at.% of Si (volume size factor to Ni: −5.81% [12]), Cu (7.18%), Ge (14.76%) and Sn (74.08%) were irradiated with fission neutrons to a dose of 0.4 dpa at 573 K by the JMTR. Well developed dislocation networks and voids are observed in the matrix of Ni, Ni–Cu and Ni–Ge as shown in Fig. 5. Only few loops and no voids are observed in Ni–Si and Ni–Sn. Pure Ni, Ni–Cu and Ni–Ge do not form loops near GB, and loops and voids in the matrix are observed by TEM. The example of Ni is shown in Fig. 6. These observations correspond to (b) in Fig. 4 of the reaction kinetics analysis. As no loops are observed near GB, (a) is not adopted, which means that the movement of interstitial clusters is essential for this defect structural evolution near GB in Ni, Ni–Cu and Ni–Ge. No voids are formed and only interstitial type dislocation loops are observed near GB in Ni–Si and Ni–Sn. Fig. 7 shows an example for Ni–Sn, which corresponds to (c) in Fig. 4, where no movement of interstitial clusters are introduced. Therefore these observations indicate that the movement of interstitial clusters and the void growth have a strong relationship.

4.2. Dislocation loops near edge dislocations

Decoration of interstitial type dislocation loops was often observed near edge dislocations [13,14]. These loops are evidence for the movement of interstitial

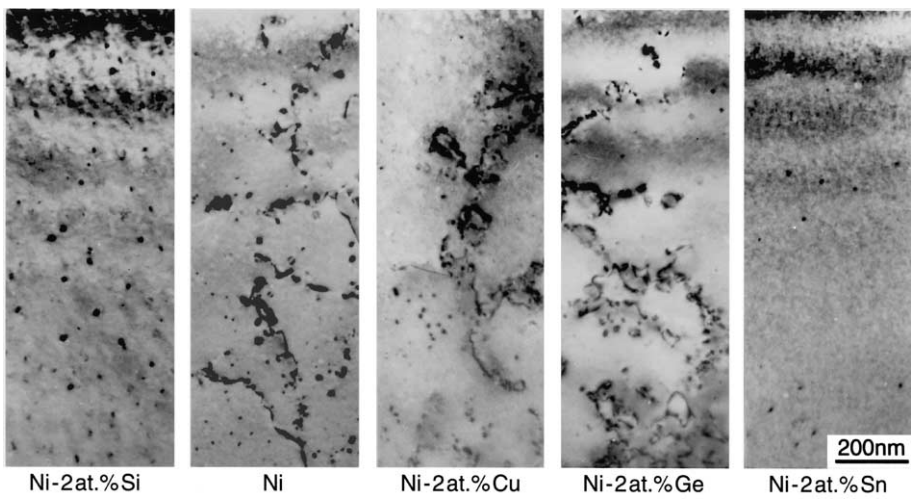

Fig. 5. Difference of defect structures in bulk Ni and Ni alloys after fission neutron irradiation in the JMTR at 573 K to 0.11 dpa.

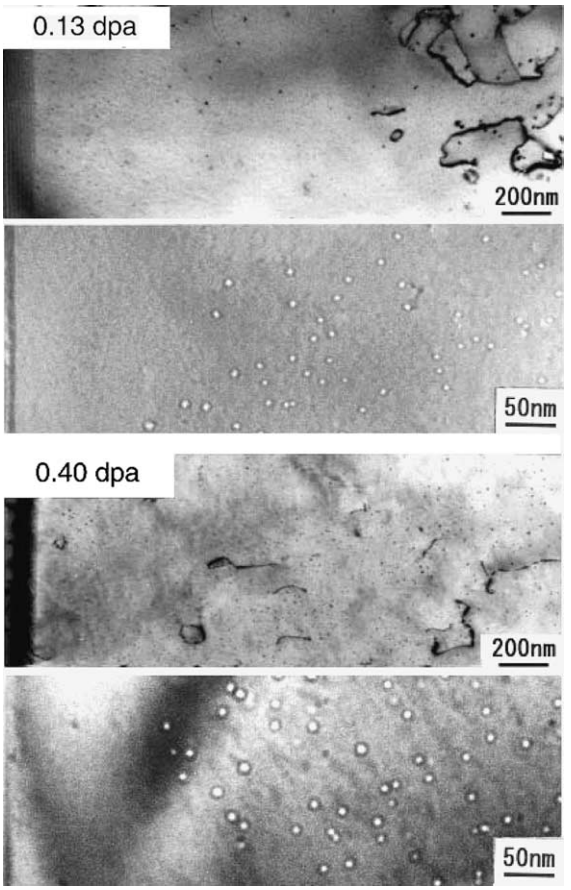

Fig. 6. Defect structures (upper: dislocation image, lower: void image in each irradiation dose) near GB (left side) in bulk Ni after fission neutron irradiation in the JMTR at 573 K.

clusters [15]. In neutron irradiated Ni, Ni–Cu and Ni–Ge at 573 K, these loops were observed. Conversely no loops were observed, however, in Ni–Si and Ni–Sn as already reported [13]. Table 1 shows the relationship between void growth and one-dimensional motion of interstitial clusters in Ni and Ni alloys at 573 K. The last column (1-D motion) is inferred by the experimental

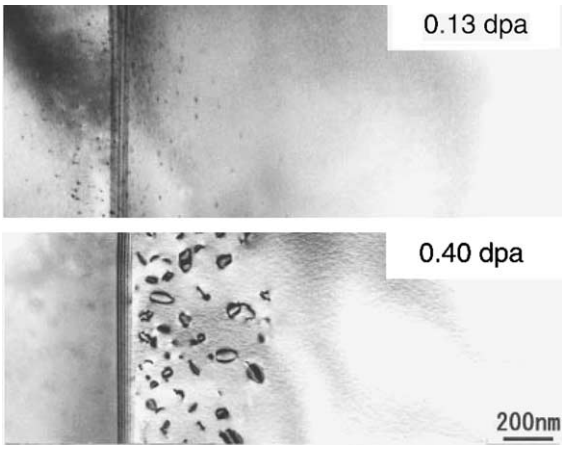

Fig. 7. Defect structures near GB (left side) in bulk Ni–2 at.% Sn after fission neutron irradiation in the JMTR at 573 K.

results. Good coincidence of one-dimensional motion and void growth can be seen.

On the other hand, in the case of Cu, the situation is different. Interstitial type dislocation loops near edge dislocations are observed in neutron irradiated Cu at 473 K as shown in Fig. 8. Voids are not observed, however, at this temperature. They are observed at 573 K as shown in Fig. 9, where no decolation of loops are observed. Loops are absorbed by dislocations easily at temperatures above 573 K. It means that the movement of interstitial clusters alone is not enough for voids growth. Clustering process of vacancies is another important factor for void growth.

5. Detection of freely migrating defects in Ni using the growth of helical dislocations

Jogs of screw dislocations form edge dislocations. If they absorb one type of point defects, the jogs climb and turn into helical dislocations as demonstrated in a book [16]. The diameter of helical dislocations after neutron irradiation represents the difference of the total number

Table 1
The correlation between void formation and inferred one dimensional (1-D) motion of interstitial clusters in Ni and Ni alloys for fission neutron irradiated Ni at 573 K

Specimens	Voids	Loops	Loops near GB	Loops near dislocations	1-D motion
Ni–2 at.% Si	×	○	○	×	×
Ni	○	○	×	○	○
Ni–2 at.% Cu	○	○	×	○	○
Ni–2 at.% Ge	○	○	×	○	○
Ni–2 at.% Sn	×	○	○	×	×

The ○ denotes the presence of the feature, and × denotes its absence.

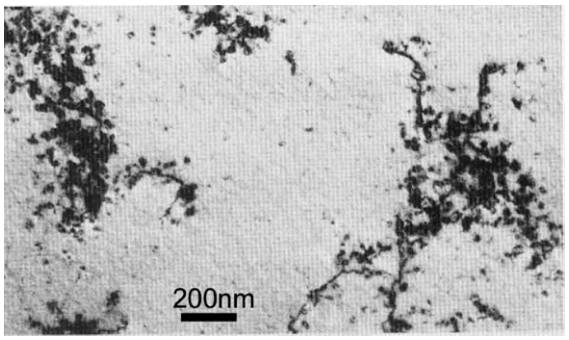

Fig. 8. Defect structures near dislocations in bulk Cu after fusion neutron irradiation in the RTNS-II to 0.017 dpa at 473 K.

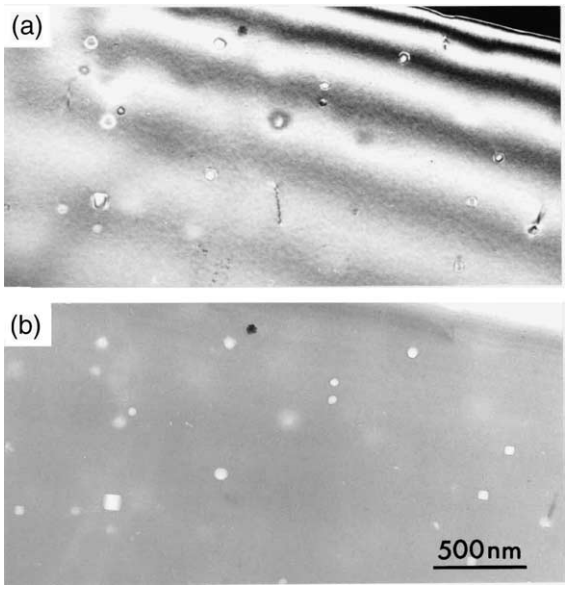

Fig. 9. Defect structures in bulk Cu after fission neutron irradiation in the JMTR to 0.14 dpa at 573 K. (a) Dislocation image and (b) void image.

of two types of point defects absorbed. In order to study the difference of freely migrating defects between fission neutron irradiation and fusion neutron irradiation, Ni was irradiated as a bulk specimen as shown in Fig. 10. The diameter of the helical dislocations was measured as a function of displacement damage as shown in Fig. 11. The increase of diameter is proportional to the displacement damage measured by dpa. There does not appear to be any effects of cascade size (fission vs. fusion neutrons). This can be explained as follows. The large cascade is divided into subcascades. Usually we consider that the formation of defects in energetic displacement

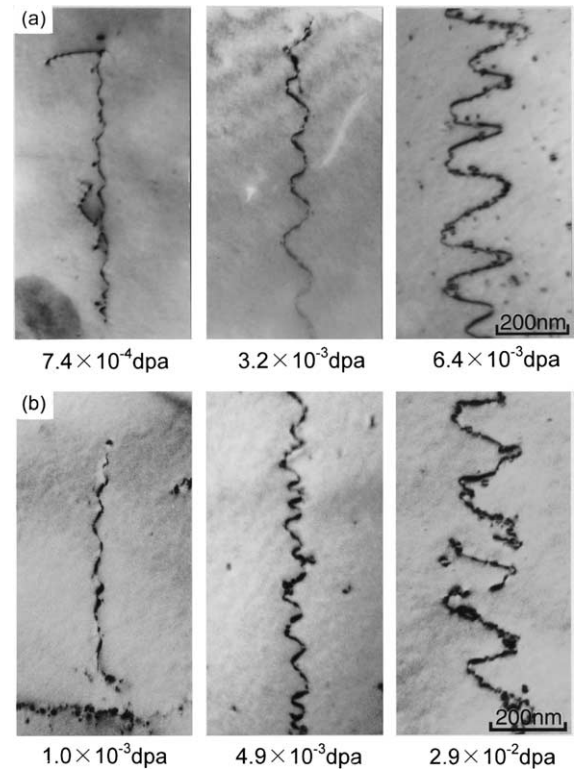

Fig. 10. Growth of helical dislocations in bulk Ni: (a) after fusion neutron irradiation in the RTNS-II at 563 K and (b) after fission neutron irradiation in the JMTR at 573 K.

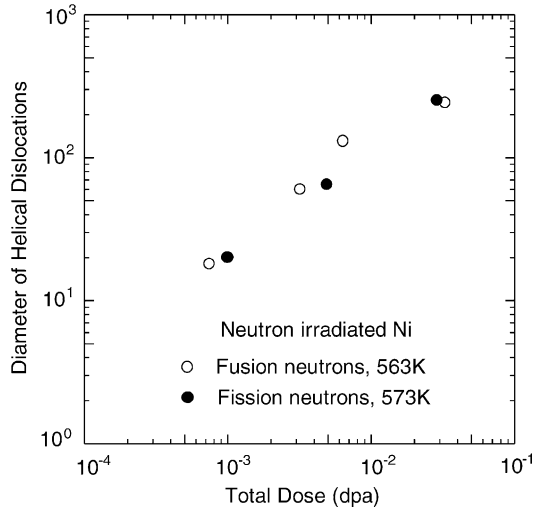

Fig. 11. The change of diameter of helical dislocations as a function of displacement damage in Ni.

cascades consists of a number of subcascades. The number of subcascades N_{SC} is expressed as

Table 2
Threshold energy for subcascade formation and the number of subcascades in fusion and fusion neutron irradiated Ni

Threshold energy for subcascade formation (keV)	The number of subcascades (1/dpa)	
	Fusion neutrons	Fission neutrons
1	3.0×10^{-2}	2.9×10^{-2}
10	3.0×10^{-3}	2.6×10^{-3}
20	1.5×10^{-3}	1.2×10^{-3}
50	5.8×10^{-4}	3.4×10^{-4}
100	2.8×10^{-4}	1.1×10^{-5}
500	2.9×10^{-5}	9.7×10^{-7}

$$N_{SC} = \int n_{SC}(E_R)\frac{d\sigma(E_R)}{dE_R}\,dE_R$$
$$n_{SC}(E_R) = \begin{cases} 0, & E_D(E_R) < E_{SC}, \\ 1, & E_{SC} \leqslant E_D(E_R) < 2E_{SC}, \\ \frac{E_D(E_R)}{2E_{SC}}, & 2E_{SC} \leqslant E_D(E_R), \end{cases} \quad (4)$$

where E_D and E_{SC} are the damage energy and the threshold energy for subcascade formation, respectively [17]. Table 2 shows the number of the subcascades per dpa in Ni as a function of E_{SC} in fusion neutron irradiation and fission neutron irradiation calculated with Specter code [2]. If the subcascade energy is below 20 keV, the number of subcascades is roughly proportional to the displacement damage measured by dpa. In the case of Ni, the subcascade energy is calculated to be 10 keV [18]. It is concluded that the same number of freely migrating defects is generated from each subcascade in fission and fusion neutron irradiated Ni.

6. Concluding remarks

In this paper, defect structural evolution in fcc metals using pre-existing defects was discussed. Electron microscopy is one of the important techniques to reveal the defect structures. However, we observe defect structures only after irradiation. In order to analyze point defect processes during irradiation, the use of pre-existing defects is a powerful technique. Though we did not discuss in this paper, interstitial type dislocation loops, voids and precipitates are possible to be used as pre-existing defects in order to obtain more information about defect structural evolution during irradiation.

Acknowledgements

The authors wish to express their most sincere gratitude to the late Professor Michio Kiritani. Without his support, encouragement and physical insight, our work could not have progressed. This work has been carried out in part by using facilities of the Irradiation Experimental Facility, Institute for Materials Research, Tohoku University.

References

[1] M. Kiritani, T. Yoshiie, S. Kojima, Y. Satoh, Radiat. Eff. Defect Solids 113 (1990) 75.
[2] L.R. Greenwood, R.K. Smither, ANL/FPP/TM-197, Argonne National Laboratory, 1985.
[3] M. Kiritani, T. Yoshiie, S. Kojima, Y. Satoh, K. Hamada, J. Nucl. Mater. 174 (1990) 327.
[4] B.N. Singh, H. Trinkaus, C.H. Woo, J. Nucl. Mater. 212–215 (1994) 168.
[5] M. Kiritani, J. Nucl. Mater. 251 (1997) 237.
[6] S.I. Golubov, B.N. Singh, H. Trinkaus, J. Nucl. Mater. 276 (2000) 78.
[7] E. Kuramoto, J. Nucl. Mater. 276 (2000) 143.
[8] H. Trinkaus, B. Singh, A.J.E. Foreman, J. Nucl. Mater. 249 (1997) 91.
[9] S.L. Dudarev, Phys. Rev. B 62 (2000) 9325.
[10] T. Yoshiie, S. Kojima, Y. Satoh, K. Hamada, M. Kiritani, J. Nucl. Mater. 191–194 (1992) 1160.
[11] T. Yoshiie, T. Ishizaki, Q. Xu, Y. Satoh, M. Kiritani, J. Nucl. Mater. 307–311 (2002) 924.
[12] H.W. King, J. Mater. Sci. 1 (1966) 79.
[13] S. Kojima, T. Yoshiie, M. Kiritani, J. Nucl. Mater. 155–157 (1988) 1249.
[14] T. Yoshiie, M. Kiritani, J. Nucl. Mater. 271–272 (1999) 296.
[15] H. Trinkaus, B.N. Singh, A.J.E. Foreman, J. Nucl. Mater. 249 (1997) 91.
[16] J.P. Hirth, J. Lothe, Theory of Dislocations, 2nd Ed., Krieger, Malabar, FL, 1992, p. 626.
[17] T. Yoshiie, X. Xu, Q. Xu, S. Yanagita, Y. Satoh, ASTM STP 398 (2001) 625.
[18] Y. Satoh, S. Kojima, T. Yoshiie, M. Kiritani, J. Nucl. Mater. 179–181 (1991) 901.